Journal of Physics: Condensed Matter

# FP-LAPW investigations of $SrS_{1-x}Se_x$, $SrS_{1-x}Te_x$ and $SrSe_{1-x}Te_x$ ternary alloys

To cite this article: S Labidi *et al* 2008 *J. Phys.: Condens. Matter* **20** 445213





J. Phys.: Condens. Matter **20** (2008) 445213 (9pp) doi:10.1088/0953-8984/20/44/445213

# FP-LAPW investigations of $SrS_{1-x}Se_x$, $SrS_{1-x}Te_x$ and $SrSe_{1-x}Te_x$ ternary alloys

**S Labidi[1], H Meradji[1], S Ghemid[1], M Labidi[1] and F El Haj Hassan[2,3]**

[1] Laboratoire de Physique des Rayonnements, Département de Physique, Faculté des Sciences, Université de Annaba, Algeria
[2] Université Libanaise, Faculté des Sciences (1), Laboratoire de Physique des Matériaux, Elhadath, Beirut, Lebanon

E-mail: hassan.f@ul.edu.lb

Received 7 July 2008, in final form 15 September 2008
Published 10 October 2008
Online at stacks.iop.org/JPhysCM/20/445213

**Abstract**

The *ab initio* full potential linearized augmented plane wave (FP-LAPW) method within density functional theory (DFT) was applied to study the effect of composition on the structural, electronic, optical and thermodynamic properties of $SrS_{1-x}Se_x$, $SrS_{1-x}Te_x$ and $SrSe_{1-x}Te_x$ ternary alloys. For exchange–correlation energy and corresponding potential, the generalized gradient approximation (GGA) by Perdew–Burke–Ernzerhof (PBE) and Engel–Vosko (EVGGA) have been used. Deviation of the lattice constants from Vegard's law and the bulk modulus from linear concentration dependence (LCD) were observed for the three alloys. The microscopic origins of the gap bowing were explained by using the approach of Zunger and co-workers. The refractive index and optical dielectric constant for the alloys of interest are calculated by using different models. In addition the thermodynamic stability of the alloys was investigated by calculating the critical temperatures of alloys.

## 1. Introduction

The strontium chalcogenides SrX (X = S, Se and Te), together with other alkaline earth chalcogenides form a very important closed shell ionic system with the NaCl crystal structure at normal conditions. They are technologically important materials, with applications in the area of luminescent devices, radiation dosimetry, fast high-resolution optically stimulated luminescence imaging, and infrared sensitive devices [1–3]. Under higher pressure prior to metallization, they undergo a first order structural phase transition to the CsCl structure [4]. Semiconductor alloys, which are solid solutions of two or more semiconducting elements, have important technological applications, especially in the manufacture of electronic and electro-optical devices [5]. One of the easiest ways to change artificially the electronic and optical properties of semiconductors is by forming their alloys. It is possible to combine two different compounds with different optical band gaps and different rigidities in order to obtain a new material with intermediate properties.

There are a number of theoretical works on these compounds concerning electronic band structure, structural phase stability, elastic properties, metallization process and optical properties [6–14]. For the band gap results, there are some discrepancies between different calculations. The band gap of SrSe is predicted to be direct by Pandey *et al* [11] and indirect by Marinelli *et al* [8]. Recently, Dadsetani and Pourghazi [15] have calculated the optical properties of SrS, SrSe and SrTe compounds using the full potential linearized augmented plane wave method (FP-LAPW). To the best of our knowledge no experimental or theoretical investigations of their ternary alloys have been appeared in the literature, therefore, the purpose of this paper is to study the structural, electronic, optical and thermodynamic properties as well as to investigate the disorder effects in these strontium alloys using the full potential linearized augmented plane wave (FP-LAPW) method.

The physical origins of gap bowing are investigated by following the approach of Zunger and co-workers [16]. This model is capable of taking into account the dominant effects of both chemical and bond length variations, unlike traditional methods like the VCA.

[3] Author to whom any correspondence should be addressed.

 

The paper is organized as follows: in the next section we give a brief description of the computational details. In section 3, the results and discussion for structural, electronic, optical and thermodynamic properties of $SrS_{1-x}Se_x$, $SrS_{1-x}Te_x$ and $SrSe_{1-x}Te_x$ alloys have been given. Finally, we present our conclusions.

## 2. Method of calculation

Describing random alloys by periodic structures will clearly introduce spurious correlations beyond a certain distance ('periodicity errors'). Preventing this problem needs a very large supercell. However, many physical properties of solids are characterized by microscopic length scales and local randomness of alloys, and modifying the large scale randomness of alloys does not affect them. Zunger *et al* [16] implemented this fact to construct a 'special quasirandom structures' (SQS) approach by the principle of close reproduction of the perfectly random network for the first few shells around a given site, deferring periodicity errors to more distant neighbours. They argued that this approach, which we have adopted in our calculation, effectively reduces the size of the supercell for studying many properties of random alloys.

The calculations were performed using the full potential linear augmented plane wave (FP-LAPW) method within the framework of density functional theory (DFT) [17, 18] as implemented in the wien2k code [19]. The exchange–correlation potential for structural and optical properties was calculated by the generalized gradient approximation (GGA) based on Perdrew *et al* [20], while for electronic properties, in addition to GGA correction, the Engel and Vosko GGA (EVGGA) [21] scheme was also applied. In the FP-LAPW method, the wavefunction, charge density and potential are expanded differently in the two regions of unit cell. Inside the non-overlapping spheres of radius $R_{MT}$ around each atom, a spherical harmonics expansion is used,

$$V(r) = \sum_{lm} V_{lm}(r) Y_{lm}(\hat{r}) \tag{1}$$

and outside the sphere (interstitial region) a plane wave basis set is chosen,

$$V(r) = \sum_{K} V_K e^{iKr} \tag{2}$$

where $Y_{lm}(\hat{r})$ is a linear combination of radial functions times spherical harmonics. Within this calculational scheme, there are no shape approximations to the charge density or potential. In the present calculation, a cubic super cell that is composed of eight atoms (four Sr atoms and four shared out between Se and Te) is considered. We use a parameter $R_{MT}K_{max} = 8$ which determines the matrix size, where $R_{MT}$ denotes the smallest atomic sphere radius and $K_{max}$ gives the magnitude of the largest $K$ vector in the plane wave expansion. The charge density was Fourier expanded up to $G_{max} = 14(\text{Ryd})^{1/2}$. The maximum $l$ values for the wavefunction expansion inside the spheres was confined to $l_{max} = 10$. We chose the muffin-tin radius of Sr, S, Se and Te to be 2.2, 2.1, 2.2 and 2.4 au respectively. A mesh of 47 special $k$-points for binary compounds and 125 special $k$-points for alloys were taken in the irreducible wedge of the Brillouin zone for the total energy calculation. Both the plane wave cut-off and the number of $k$-points were varied to ensure total energy convergence.

## 3. Results and discussion

### *3.1. Structural properties*

Firstly, the structural properties of the binary compounds SrS, SrSe and SrTe in the rocksalt structure were analysed. We model the alloys at some selected compositions with ordered structures described in terms of periodically repeated supercells with eight atoms per unit cell, for the compositions $x = 0.25, 0.5, 0.75$. For the structures considered, the total energies were calculated as a function of volume and were fitted to Murnaghan's equation of state [22]. The corresponding equilibrium lattice constants and bulk modulus for both binary compounds and their alloys are given in table 1. Considering the general trend that the GGA usually overestimates the lattice parameters [23], our GGA results for the binary compounds are in reasonable agreement with the experimental and other theoretical values. Usually, in the treatment of alloy problems, it is assumed that the atoms are located at ideal lattice sites and the lattice constants of alloys should vary linearly with composition $x$ according to Vegard's law [24], however, violations of Vegard's rule have been reported in semiconductor alloys both experimentally [25] and theoretically [26].

A small deviation from Vegard's law is clearly visible for the $SrS_{1-x}Se_x$, $SrS_{1-x}Te_x$ and $SrSe_{1-x}Te_x$ alloys with upward bowing parameters equal to $-0.043$, $-0.110$ and $-0.031$ Å respectively, obtained by fitting the calculated values with a polynomial function. The physical origin of this small deviation should be mainly due to the weak mismatches of the lattice constants of binary compounds SrX. However, the value of the bowing parameter for $SrS_{1-x}Te_x$ alloy is relatively higher.

The composition dependence of bulk modulus is compared with the results predicted by linear concentration dependence (LCD). A significant deviation of the bulk modulus from the linear concentration dependence with upward bowing equal to $-4.706$ GPa for $SrS_{1-x}Se_x$ alloy was observed, while for $SrS_{1-x}Te_x$ and $SrSe_{1-x}Te_x$, we obtained an downward bowing parameter equal to 6.930 and 8.937 GPa, respectively. Our results show that the bulk modulus decreases with an increase of the Se and Te concentration $x$. This suggests that as $x$ increases from $x = 0$ to 1 the alloys become generally more compressible.

### *3.2. Electronic properties*

To compute the band gaps for strontium chalcogenide compounds and their alloys, self-consistently GGA and EVGGA are used within DFT.

The calculated band structure energies indicate an indirect band gap (Γ–X). The results are given in table 2. The band gap values given by EVGGA formalism are reasonably in agreement with experiment and GGA gives lower value. In

**Table 1.** Calculated lattice parameter ($a$) and bulk modulus $B$ of for strontium chalcogenides and their alloys at equilibrium volume.

| | | Lattice constant $a$ (Å) | | | Bulk modulus $B$ (GPa) | | |
|---|---|---|---|---|---|---|---|
| | $x$ | This work | Experiment | Other calculations | This work | Experiment | Other calculations |
| $SrS_{1-x}Se_x$ | 1 | 6.303 | 6.236 [4] | 6.323 [7] | 41.1 | 45 [4] | 41 [7] |
| | 0.75 | 6.251 | | | 43.5 | | |
| | 0.5 | 6.195 | | | 44.8 | | |
| | 0.25 | 6.133 | | | 45.6 | | |
| | 0 | 6.065 | 6.024 [27] | 6.076 [7] | 46.3 | 58 [27] | 47 [7] |
| $SrS_{1-x}Te_x$ | 1 | 6.735 | 6.66 [13] | 6.76 [7] | 31.8 | 39.5 [13] | 36 [7] |
| | 0.75 | 6.596 | | | 33.5 | | |
| | 0.5 | 6.417 | | | 37.5 | | |
| | 0.25 | 6.267 | | | 41.6 | | |
| | 0 | 6.065 | 6.024 [27] | 6.076 [7] | 46.3 | 39.5 [13] | 36 [7] |
| $SrSe_{1-x}Te_x$ | 1 | 6.735 | 6.66 [13] | 6.76 [7] | 31.8 | 39.5 [13] | 36 [7] |
| | 0.75 | 6.641 | | | 32.0 | | |
| | 0.5 | 6.525 | | | 34.0 | | |
| | 0.25 | 6.412 | | | 38.1 | | |
| | 0 | 6.303 | 6.236 [4] | 6.323 [7] | 41.1 | 45 [4] | 41 [7] |

fact, it is well known that the GGA usually underestimates the experimental energy band gap [28, 29]. In fact, the energy gaps are systematically underestimated in *ab initio* calculations and that this is an intrinsic feature of density functional theory (DFT), DFT being a ground-state theory not suitable for describing excited-state properties, such as the energy gap. However, it is widely accepted that GGA (LDA) electronic band structures are qualitatively in good agreement with experiments as regards the ordering of the energy levels and the shape of the bands. Engel and Vosko [21] by considering the underestimation of the energy gap constructed a new functional form of the GGA which is able to reproduce better the exchange potential at the expense of less agreement in exchange energy. This approach (EVGGA) yields a better band splitting. However, in this method, the quantities that depend on an accurate description of exchange energy $E_x$, such as equilibrium volumes, are in poor agreement with experiment. We have optimized the structural parameters for both schemes to be able to confirm our result, this is consistent with the results reported by El Haj Hassan *et al* [26, 30].

Figure 1 shows the composition dependence of the calculated band gaps using GGA and EVGGA schemes. We calculated the total bowing parameter by fitting the nonlinear variation of calculated band gaps versus concentration with quadratic function. The results obey the following variations:

$$SrS_{1-x}Se_x \Rightarrow \begin{cases} E_g^{GGA}(x) = 2.535 - 0.311x + 0.043x^2, \\ E_g^{EVGGA}(x) = 3.395 - 0.376x + 0.038x^2, \end{cases} \quad (3)$$

$$SrS_{1-x}Te_x \Rightarrow \begin{cases} E_g^{GGA}(x) = 2.539 - 1.321x + 0.601x^2, \\ E_g^{EVGGA}(x) = 3.395 - 1.630x + 0.801x^2, \end{cases} \quad (4)$$

$$SrSe_{1-x}Te_x \Rightarrow \begin{cases} E_g^{GGA}(x) = 2.265 - 0.727x + 0.276x^2, \\ E_g^{EVGGA}(x) = 3.067 - 0.838x + 0.332x^2. \end{cases} \quad (5)$$

The results of the calculated gap bowing are given in table 3. It is clearly seen that the calculated band gap exhibits weak composition dependence for $SrS_{1-x}Se_x$ alloy while the gap bowing for $SrS_{1-x}Te_x$ and $SrSe_{1-x}Te_x$ is found to be much higher than the corresponding value for $SrS_{1-x}Se_x$.

**Table 2.** Gap energy $E_g$ of the strontium compounds and their alloys at equilibrium volume.

| | | $E_g$ (eV) | | | |
|---|---|---|---|---|---|
| | | This work | | | |
| | $x$ | GGA | EVGGA | Experiment | Other work |
| $SrS_{1-x}Se_x$ | 1 | 2.266 | 3.065 | 3.81 [34] | 2.19 [7] 2.26 [35] |
| | 0.75 | 2.332 | 3.121 | | |
| | 0.5 | 2.386 | 3.218 | | |
| | 0.25 | 2.462 | 3.317 | | |
| | 0 | 2.536 | 3.389 | 4.32 [34] | 2.45 [7] 2.68 [35] |
| $SrS_{1-x}Te_x$ | 1 | 1.807 | 2.554 | | 1.73 [7] 1.89 [35] |
| | 0.75 | 1.926 | 2.668 | | |
| | 0.5 | 1.982 | 2.723 | | |
| | 0.25 | 2.270 | 3.071 | | |
| | 0 | 2.536 | 3.389 | 4.32 [34] | 2.45 [7] 2.68 [35] |
| $SrSe_{1-x}Te_x$ | 1 | 1.807 | 2.554 | | 1.73 [7] 1.89 [35] |
| | 0.75 | 1.896 | 2.649 | | |
| | 0.5 | 1.951 | 2.703 | | |
| | 0.25 | 2.106 | 2.892 | | |
| | 0 | 2.266 | 3.065 | 3.81 [34] | 2.19 [7] 2.26 [35] |

It has been seen that the main influence of the band gap energy is due to the lattice constant and the electronegativity mismatch of the parent atoms [31, 32]. In order to better understand the physical origins of the gap bowing in these alloys, we follow the procedure of Bernard and Zunger [33], in which the bowing parameter ($b$) is decomposed into three physically distinct contributions. The overall gap bowing coefficient at $x = 0.5$ measures the change in band gap according to the reaction:

$$AB\,(a_{AB}) + AC\,(a_{AC}) \rightarrow AB_{0.5}C_{0.5}\,(a_{eq}) \quad (6)$$

where $a_{AB}$ and $a_{AC}$ are the equilibrium lattice constants of the binary compounds AB and AC, respectively, and $a_{eq}$ is the alloy equilibrium lattice constant. We now decompose

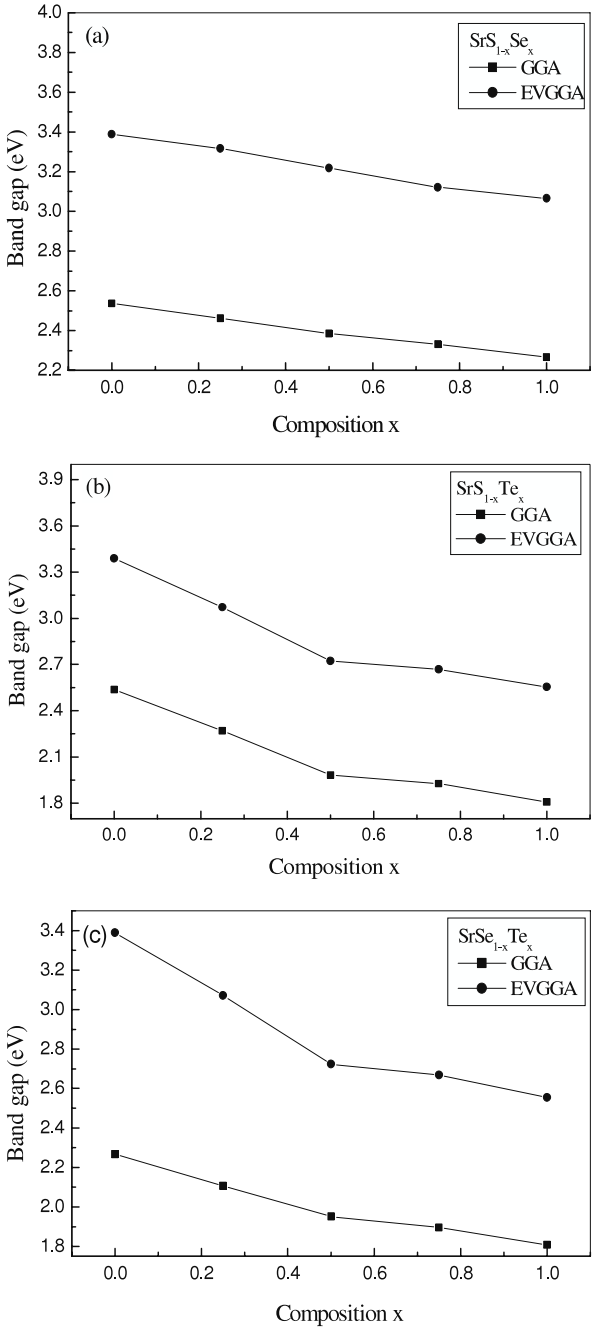


**Figure 1.** Composition dependence of the calculated band gap using GGA (solid squares) and EVGGA (solid circles) for (a) $SrS_{1-x}Se_x$, (b) $SrS_{1-x}Te_x$ and (b) $SrSe_{1-x}Te_x$ alloys.

reaction (6) into three steps:

$$\mathrm{AB}\,(a_{\mathrm{AB}}) + \mathrm{AC}\,(a_{\mathrm{AC}}) \xrightarrow{\mathrm{VD}} \mathrm{AB}\,(a) + \mathrm{AC}\,(a)\,, \tag{7}$$

$$\mathrm{AB}\,(a) + \mathrm{AC}\,(a) \xrightarrow{\mathrm{CE}} \mathrm{AB_{0.5}C_{0.5}}\,(a)\,, \tag{8}$$

$$\mathrm{AB_{0.5}C_{0.5}}\,(a) \xrightarrow{\mathrm{SR}} \mathrm{AB_{0.5}C_{0.5}}\,(a_{\mathrm{eq}})\,. \tag{9}$$

The first step measures the volume deformation (VD) effect on the bowing. The corresponding contribution $b_{\mathrm{VD}}$ to the total gap bowing parameter represents the relative response of the band structure of the binary compounds AB and AC to hydrostatic pressure, which here arises from the change of their individual equilibrium lattice constants to the alloy value $a = a(x)$ (from Vegard's rule). The second contribution, the charge exchange (CE) contribution $b_{\mathrm{CE}}$, reflects a charge transfer effect which is due to the different (averaged) bonding behaviour at the lattice constant $a$. The final step measures changes due to the structural relaxation (SR) in passing from the unrelaxed to the relaxed alloy by $b_{\mathrm{SR}}$.

**Table 3.** Decomposition of the optical bowing into volume deformation (VD), charge exchange (CE), and structural relaxation (SR) contributions compared with that obtained by a quadratic fit and other predictions (all values are in eV).

| | | This work | | | |
|---|---|---|---|---|---|
| | | Zunger approach | | Quadratic fits | |
| | | GGA | EVGGA | GGA | EVGGA |
| $SrS_{1-x}Se_x$ | $b_{\mathrm{VD}}$ | 0.352 | 0.078 | | |
| | $b_{\mathrm{CE}}$ | −0.256 | −0.014 | | |
| | $b_{\mathrm{SR}}$ | −0.036 | −0.028 | | |
| | $b$ | 0.060 | 0.036 | 0.043 | 0.038 |
| $SrS_{1-x}Te_x$ | $b_{\mathrm{VD}}$ | 0.398 | 0.514 | | |
| | $b_{\mathrm{CE}}$ | 0.428 | 0.528 | | |
| | $b_{\mathrm{SR}}$ | −0.068 | −0.048 | | |
| | $b$ | 0.758 | 0.994 | 0.601 | 0.801 |
| $SrSe_{1-x}Te_x$ | $b_{\mathrm{VD}}$ | 0.170 | 0.245 | | |
| | $b_{\mathrm{CE}}$ | 0.192 | 0.198 | | |
| | $b_{\mathrm{SR}}$ | −0.020 | −0.020 | | |
| | $b$ | 0.342 | 0.426 | 0.276 | 0.332 |

Consequently, the total gap bowing parameter is defined as:

$$b = b_{\mathrm{VD}} + b_{\mathrm{CE}} + b_{\mathrm{SR}} \tag{10}$$

$$b_{\mathrm{VD}} = 2\left[\varepsilon_{\mathrm{AB}}\,(a_{\mathrm{AB}}) - \varepsilon_{\mathrm{AB}}\,(a) + \varepsilon_{\mathrm{AC}}\,(a_{\mathrm{AC}}) - \varepsilon_{\mathrm{AC}}\,(a)\right] \tag{11}$$

$$b_{\mathrm{CE}} = 2\left[\varepsilon_{\mathrm{AB}}\,(a) + \varepsilon_{\mathrm{AC}}\,(a) - 2\varepsilon_{\mathrm{ABC}}\,(a)\right] \tag{12}$$

$$b_{\mathrm{SR}} = 4\left[\varepsilon_{\mathrm{ABC}}\,(a) - \varepsilon_{\mathrm{ABC}}\left(a_{\mathrm{eq}}\right)\right] \tag{13}$$

where $\varepsilon$ is the energy gap which has been calculated for the indicated atomic structures and lattice constants. The energy gaps terms in equations (11)–(13) are calculated separately with a self-consistent band structure approach. The results are given in table 3. It can be seen that the calculated quadratic parameters (gap bowing) within GGA and EVGGA are very close to their corresponding results obtained by the Zunger approach. The total gap bowing of $SrS_{1-x}Te_x$ alloy is more important than that of the other alloys. The contribution of the volume deformation term to the bowing parameter $b_{\mathrm{VD}}$ has been found to be significant for $SrS_{1-x}Te_x$. This term is correlated to the relative large mismatch of the lattice constants of the corresponding binary compounds compared to those constituting the $SrS_{1-x}Se_x$ and $SrSe_{1-x}Te_x$ alloys. The charge transfer effect is also significant for $SrS_{1-x}Te_x$ and $SrSe_{1-x}Te_x$ alloys. It is due to the electronegativity difference between S(2.58), Se(2.55) and Te(2.1) atoms. The contribution of the structural relaxation is small.

**Table 4.** Refractive indices of $SrS_{1-x}Se_x$, $SrS_{1-x}Te_x$ and $SrSe_{1-x}Te_x$ for different compositions $x$.

| | | This work | | | | | |
|---|---|---|---|---|---|---|---|
| | $x$ | FP-LAPW | Relation 16 | Relation 17 | Relation 18 | Experiment | Other calculations |
| $SrS_{1-x}Se_x$ | 1 | 2.244 | 2.627 | 2.679 | 2.600 | 2.21 [40, 41] | 2.15 [39] |
| | 0.75 | 2.239 | 2.608 | 2.638 | 2.574 | | |
| | 0.5 | 2.230 | 2.593 | 2.604 | 2.554 | | |
| | 0.25 | 2.224 | 2.573 | 2.557 | 2.526 | | |
| | 0 | 2.217 | 2.554 | 2.511 | 2.499 | 2.10 [40, 41] | 2.11 [39] |
| $SrS_{1-x}Te_x$ | 1 | 2.448 | 2.780 | 2.963 | 2.796 | 2.41 [40, 41] | 2.29 [39] |
| | 0.75 | 2.367 | 2.736 | 2.889 | 2.742 | | |
| | 0.5 | 2.316 | 2.716 | 2.855 | 2.717 | | |
| | 0.25 | 2.268 | 2.626 | 2.676 | 2.598 | | |
| | 0 | 2.217 | 2.554 | 2.511 | 2.499 | 2.10 [40, 41] | 2.11 [39] |
| $SrSe_{1-x}Te_x$ | 1 | 2.448 | 2.780 | 2.963 | 2.796 | 2.41 [40, 41] | 2.29 [39] |
| | 0.75 | 2.335 | 2.747 | 2.889 | 2.755 | | |
| | 0.5 | 2.291 | 2.728 | 2.874 | 2.731 | | |
| | 0.25 | 2.252 | 2.676 | 2.778 | 2.664 | | |
| | 0 | 2.244 | 2.627 | 2.679 | 2.600 | 2.21 [40, 41] | 2.15 [39] |

### *3.3. Optical properties*

Optical properties of a solid are usually described in terms of the complex dielectric function $\varepsilon(\omega) = \varepsilon_1(\omega) + i\varepsilon_2(\omega)$. The imaginary part of the dielectric function in the long wavelength limit cam be obtained directly from the electronic structure calculation, using the joint density of states and the optical matrix elements. The real part of the dielectric function can be derived from the imaginary part by the Kramers–Kronig relationship. The knowledge of both the real and the imaginary parts of the dielectric function allows the calculation of important optical functions. The refractive index $n(\omega)$ is given by

$$n(\omega) = \left[\frac{\varepsilon_1(\omega)}{2} + \frac{\sqrt{\varepsilon_1^2(\omega) + \varepsilon_2^2(\omega)}}{2}\right]^{1/2}. \tag{14}$$

At low frequency ($\omega = 0$), we get the following relation:

$$n(0) = \varepsilon^{1/2}(0). \tag{15}$$

The refractive index and optical dielectric constants are very important to determine the optical and electric properties of the crystal.

Empirical relations [36–38] relate the refractive index to the energy band gap for a large set of semiconductors. The following models are used:

(i) The Moss formula [37] based on atomic model

$$E_g n^4 = k \tag{16}$$

where $E_g$ is the energy band gap and $k$ a constant. The value of $k$ is given to be 108 eV by Ravindra and Srivastava [36].

(ii) The expression proposed by Ravindra *et al* [37]

$$n = \alpha + \beta E_g \tag{17}$$

With $\alpha = 4.084$; and $\beta = -0.62\ \text{eV}^{-1}$.

(iii) Herve and Vandamme's empirical relation [38] is given by

$$n = \sqrt{1 + \left(\frac{A}{E_g + B}\right)^2} \tag{18}$$

With $A = 13.6$ eV and $B = 3.4$ eV.

In table 4, we summarize the calculated values of the refractive index for the alloys under investigation for some compositions obtained by using the FP-LAPW method and the different models. Comparison with the available data has been done.

As compared with the other relations used, it appears that the values of the refractive index obtained from FP-LAPW calculations for the end-point compounds (i.e. SrS, SrSe and SrTe) are in better agreement with available experimental results. Unfortunately, no comparison has been made for the refractive index of the alloys of interest in the $0 < x < 1$ composition range. Figure 2 shows the variation of the calculated refractive index versus concentration for $SrS_{1-x}Se_x$, $SrS_{1-x}Te_x$ and $SrSe_{1-x}Te_x$ alloys. The refractive index increases monotonically with increasing Se or Te content over the entire range of 0–1. The calculated refractive indices versus concentration were fitted by a polynomial equation. The results are summarized as follows:

$$SrS_{1-x}Se_x \Rightarrow \begin{cases} n_1(x) = 2.216 + 0.028x - 0.001x^2 \\ \quad \text{(FP-LAPW)}, \\ n_2(x) = 2.554 + 0.078x - 0.005x^2 \\ \quad \text{(from relation 16)}, \\ n_3(x) = 2.511 + 0.193x - 0.026x^2 \\ \quad \text{(from relation 17)}, \\ n_4(x) = 2.499 + 0.111x - 0.011x^2 \\ \quad \text{(from relation 18)}. \end{cases} \tag{19}$$

$$\mathrm{SrS}_{1-x}\mathrm{Te}_x \Rightarrow \begin{cases} n_1(x) = 2.220 + 0.152x + 0.072x^2 \\ \quad \text{(FP-LAPW)}, \\ n_2(x) = 2.552 + 0.368x - 0.144x^2 \\ \quad \text{(from relation 16)}, \\ n_3(x) = 2.508 + 0.820x - 0.373x^2 \\ \quad \text{(from relation 17)}, \\ n_4(x) = 2.496 + 0.505x - 0.210x^2 \\ \quad \text{(from relation 18)}. \end{cases} \tag{20}$$

$$\mathrm{SrSe}_{1-x}\mathrm{Te}_x \Rightarrow \begin{cases} n_1(x) = 2.246 - 0.049x + 0.245x^2 \\ \quad \text{(FP-LAPW)}, \\ n_2(x) = 2.626 + 0.225x - 0.074x^2 \\ \quad \text{(from relation 16)}, \\ n_3(x) = 2.679 + 0.450x - 0.171x^2 \\ \quad \text{(from relation 17)}, \\ n_4(x) = 2.599 + 0.294x - 0.101x^2 \\ \quad \text{(from relation 18)}. \end{cases} \tag{21}$$

For $\mathrm{SrS}_{1-x}\mathrm{Se}_x$ alloy, a marginal upward bowing is observed for $n_1(x)$ and $n_2(x)$, compared with $n_3(x)$ and $n_4(x)$. Here $n_1(x)$, $n_2(x)$, $n_3(x)$ and $n_4(x)$ are referred to as the refractive index obtained from the FP-LAPW method and relations (16)–(18), respectively.

From these equations, we can note the weak nonlinear dependence of the refractive index of the alloys with concentration $x$. Interestingly, we note on going from SrS to SrSe or SrTe, the band gap of the three alloys decreases (see figure 1) whereas, the refractive index increases. The ternary alloys show that the smaller band gap material has a larger value of the refractive index as the general behaviour of many other groups III–V semiconductors alloys [42].

The optical dielectric constant was estimated according to expression (15), the results are given in table 5. Our results obtained by the FP-LAPW method are in reasonable agreement with experimental values. Qualitatively, the compositional dependence of the dielectric function of the alloys has the same trend as that of the refractive index. This is not surprising as the dielectric function is directly calculated from relation (15).

Least-squares fit were made on our data:

$$\mathrm{SrS}_{1-x}\mathrm{Se}_x \Rightarrow \begin{cases} \varepsilon_1(x) = 4.914 + 0.124x - 0.001x^2 \\ \quad \text{(FP-LAPW)}, \\ \varepsilon_2(x) = 6.522 + 0.399x - 0.024x^2 \\ \quad \text{(from relation 16)}, \\ \varepsilon_3(x) = 6.305 + 0.972x - 0.106x^2 \\ \quad \text{(from relation 17)}, \\ \varepsilon_4(x) = 6.245 + 0.554x - 0.044x^2 \\ \quad \text{(from relation 18)}. \end{cases} \tag{22}$$

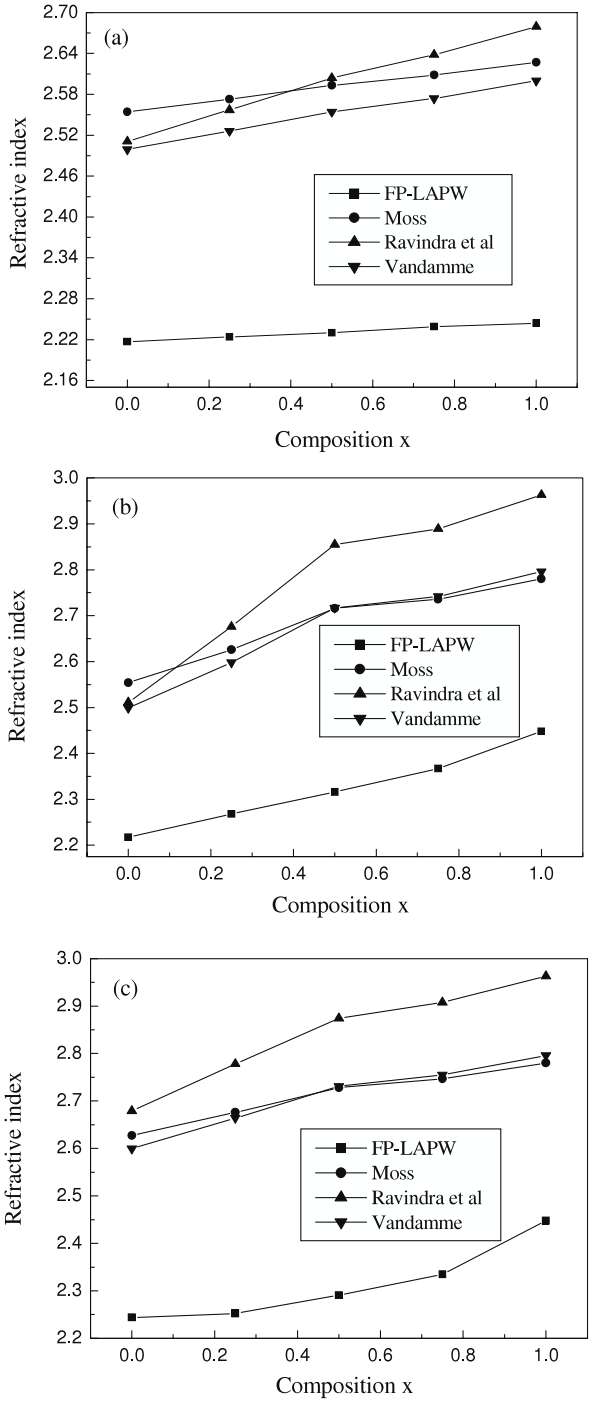


**Figure 2.** Refractive index for (a) $\mathrm{SrS}_{1-x}\mathrm{Se}_x$, (b) $\mathrm{SrS}_{1-x}\mathrm{Te}_x$ and (c) $\mathrm{SrSe}_{1-x}\mathrm{Te}_x$ alloys for different composition $x$.

$$\mathrm{SrS}_{1-x}\mathrm{Te}_x \Rightarrow \begin{cases} \varepsilon_1(x) = 4.929 + 0.653x + 0.393x^2 \\ \quad \text{(FP-LAPW)}, \\ \varepsilon_2(x) = 6.510 + 1.923x - 0.722x^2 \\ \quad \text{(from relation 16)}, \\ \varepsilon_3(x) = 6.287 + 4.327x - 1.874x^2 \\ \quad \text{(from relation 17)}, \\ \varepsilon_4(x) = 6.230 + 2.601x - 1.036x^2 \\ \quad \text{(from relation 18)}. \end{cases} \tag{23}$$

**Table 5.** Optical dielectric constants of $SrS_{1-x}Se_x$, $SrS_{1-x}Te_x$ and $SrSe_{1-x}Te_x$ for different compositions $x$.

| | | This work | | | | | |
|---|---|---|---|---|---|---|---|
| | $x$ | FP-LAPW | Relation 16 | Relation 17 | Relation 18 | Experiment | Other calculations |
| $SrS_{1-x}Se_x$ | 1 | 5.036 | 6.901 | 7.177 | 6.760 | 4.33 [43] | 5.46 [15] |
| | 0.75 | 5.013 | 6.801 | 6.959 | 6.625 | | |
| | 0.5 | 4.972 | 6.723 | 6.780 | 6.522 | | |
| | 0.25 | 4.946 | 6.620 | 6.538 | 6.380 | | |
| | 0 | 4.915 | 6.522 | 6.305 | 6.245 | 4.09 [43] | 5.20 [15] |
| $SrS_{1-x}Te_x$ | 1 | 5.993 | 7.728 | 8.779 | 7.817 | 4.91 [43] | 6.32 [15] |
| | 0.75 | 5.602 | 7.485 | 8.346 | 7.518 | | |
| | 0.5 | 5.363 | 7.376 | 8.151 | 7.382 | | |
| | 0.25 | 5.143 | 6.895 | 7.160 | 6.749 | | |
| | 0 | 4.915 | 6.522 | 6.305 | 6.245 | 4.09 [43] | 5.20 [15] |
| $SrSe_{1-x}Te_x$ | 1 | 5.993 | 7.728 | 8.779 | 7.817 | 4.91 [43] | 6.32 [15] |
| | 0.75 | 5.455 | 7.546 | 8.456 | 7.590 | | |
| | 0.5 | 5.249 | 7.436 | 8.259 | 7.458 | | |
| | 0.25 | 5.076 | 7.160 | 7.717 | 7.096 | | |
| | 0 | 5.036 | 6.901 | 7.177 | 6.760 | 4.33 [43] | 5.46 [15] |

$$SrSe_{1-x}Te_x \Rightarrow \begin{cases} \varepsilon_1(x) = 5.050 - 0.258x + 1.176x^2 \\ \qquad \text{(FP-LAPW)}, \\ \varepsilon_2(x) = 6.900 + 1.184x - 0.370x^2 \\ \qquad \text{(from relation 16)}, \\ \varepsilon_3(x) = 7.177 + 2.467x - 0.890x^2 \\ \qquad \text{(from relation 17)}, \\ \varepsilon_4(x) = 6.758 + 1.555x - 0.512x^2 \\ \qquad \text{(from relation 18)}. \end{cases} \quad (24)$$

where $\varepsilon_1(x)$, $\varepsilon_2(x)$, $\varepsilon_3(x)$ and $\varepsilon_4(x)$ stand for the optical dielectric constants estimated from the corresponding refractive indices $n_1(x)$, $n_2(x)$, $n_3(x)$ and $n_4(x)$ respectively, for a given value of $x$.

### *3.4. Thermodynamic properties*

In order to study the phase stability of $SrS_{1-x}Se_x$, $SrS_{1-x}Te_x$ and $SrSe_{1-x}Te_x$ alloys, we calculated the phase diagram based on the regular-solution model [44–46]. The Gibbs free energy of mixing, $\Delta G_m$, is expressed as

$$\Delta G_m = \Delta H_m - T\Delta S_m \quad (25)$$

where

$$\Delta H_m = \Omega x(1-x) \quad (26)$$

$$\Delta S_m = -R[x\ln x + (1-x)\ln(1-x)] \quad (27)$$

$\Delta H_m$ and $\Delta S_m$ are the enthalpy and entropy of mixing, respectively; $\Omega$ is the interaction parameter which depends on the material, $R$ the gas constant and $T$ the absolute temperature. The mixing enthalpy of alloys can be obtained from the calculated total energies as

$$\Delta H_m = E_{AB_xC_{1-x}} - xE_{AB} - (1-x)E_{AC}, \quad (28)$$

where $E_{AB_xC_{1-x}}$, $E_{AB}$ and $E_{AC}$ are the respective energies of $AB_xC_{1-x}$ alloy and the binary compounds AB and AC. We then calculated $\Delta H_m$ to obtain $\Omega$ as a function of concentration. The interaction parameter increases almost linearly with increasing $x$. From a linear fit we obtained:

$$SrS_{1-x}Se_x \Rightarrow \Omega\ (\text{kcal mol}^{-1}) = -1.733x + 1.455, \quad (29)$$

$$SrS_{1-x}Te_x \Rightarrow \Omega\ (\text{kcal mol}^{-1}) = 1.042x + 10.447, \quad (30)$$

$$SrSe_{1-x}Te_x \Rightarrow \Omega\ (\text{kcal mol}^{-1}) = 5.270x + 3.481. \quad (31)$$

The average values of the $x$-dependent $\Omega$ in the range $0 \leqslant x \leqslant 1$ obtained from these equations for $SrS_{1-x}Se_x$, $SrS_{1-x}Te_x$ and $SrSe_{1-x}Te_x$ alloys are 0.588, 10.968 and 6.116 kcal mol$^{-1}$, respectively. By calculating the free energy of mixing $\Delta G_m$ at different concentrations using equations (25)–(27), we determine the $T$–$x$ phase diagram depicting stable, metastable and unstable mixing regions of the alloy.

At a temperature lower than the critical temperature $T_c$, the two binodal points are determined as those points at which the common tangent line touches the $\Delta G_m$ curves. The two spinodal points are determined as those points at which the second derivative of $\Delta G_m$ is zero; $\partial^2(\Delta G_m)/\partial x^2 = 0$.

Figure 3 shows the calculated phase diagram including the spinodal and the binodal curves of the alloys of interest. We observed a critical temperature $T_c$ of 148, 2761 and 1540 K for $SrS_{1-x}Se_x$, $SrS_{1-x}Te_x$ and $SrSe_{1-x}Te_x$ alloys, respectively. The phase diagram shows symmetry which is due to the use of average values of $\Omega$. This result is similar to the qualitative behaviour of other alloys [47–49]. The spinodal curve in the phase diagram marks the equilibrium solubility limit, i.e., the miscibility gap. For temperatures and compositions above this curve a homogeneous alloy is predicted. The wide range between spinodal and binodal curves indicates that the alloy may exist as a metastable phase. Finally, our results indicate that the $SrS_{1-x}Se_x$ alloy is stable at low temperature while the $SrS_{1-x}Te_x$ and $SrSe_{1-x}Te_x$ alloys are stable at high temperature.

## 4. Conclusion

In conclusion, first-principles calculations were performed to investigate the structural, electronic, thermodynamic and

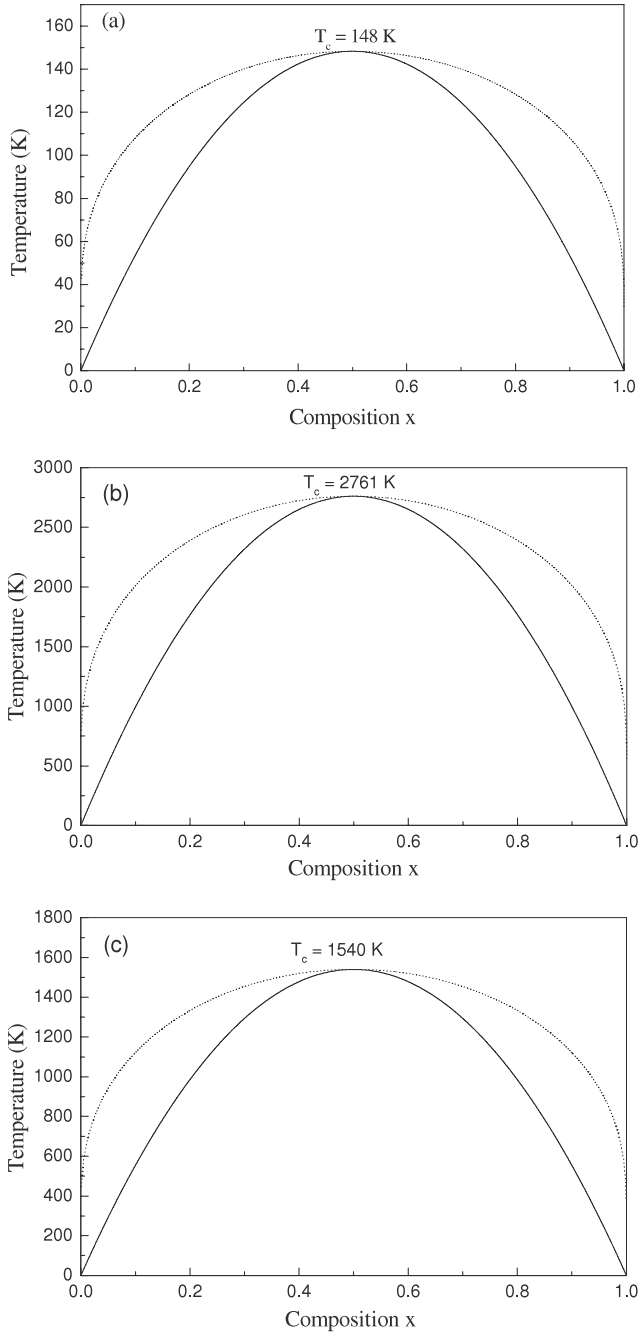


**Figure 3.** $T$–$x$ phase diagram of (a) $SrS_{1-x}Se_x$, (b) $SrS_{1-x}Te_x$ and (c) $SrSe_{1-x}Te_x$ alloys. Dashed line: binodal curve. Solid line: spinodal curve.

optical properties of $SrS_{1-x}Se_x$, $SrS_{1-x}Te_x$ and $SrSe_{1-x}Te_x$ ternary alloys. We have investigated the composition dependence of the lattice constant, bulk modulus, band gap, refractive indices, optical dielectric constants and critical temperature. The lattice constant of $SrS_{1-x}Se_x$, $SrS_{1-x}Te_x$ and $SrSe_{1-x}Te_x$ alloys exhibits a small deviation from Vegard's law with upward bowing parameters equal to $-0.043$, $-0.110$ and $-0.031$ Å, respectively. This small deviation is mainly due to the mismatches of the lattice constants of binary compounds. A significant deviation of the bulk modulus from LCD was found for $SrSe_{1-x}Te_x$, and $SrS_{1-x}Se_x$ found to be more compressible than the other two alloys. The gap bowing for $SrS_{1-x}Te_x$ alloy is found to be much higher than the corresponding value of $SrS_{1-x}Se_x$ and $SrSe_{1-x}Te_x$ alloys. The volume deformation and charge exchange contributions are found to be significant. We have calculated the dielectric functions. Further, we derived the static dielectric constant and the refractive index. The calculated phase diagrams indicate a critical temperature of 148, 2761 and 1540 K for $SrS_{1-x}Se_x$, $SrS_{1-x}Te_x$ and $SrSe_{1-x}Te_x$ alloys, respectively. It means that the $SrS_{1-x}Se_x$ alloy is stable at low temperature while the $SrS_{1-x}Te_x$ and $SrSe_{1-x}Te_x$ are stable at high temperature.

Taking into account the absence of experimental data for the alloys of interest, the reported calculations provide the first results obtained from first principles which can be useful for future investigations.

## References


[1] Nakanishi Y, Ito T, Hatanaka Y and Shimaoka G 1992 *Appl. Surf. Sci.* **66** 515
[2] Asano S, Yamashita N and Nakao Y 1978 *Phys. Status Solidi* b **89** 663
[3] Pandey R and Sivaraman S 1991 *J. Phys. Chem. Solids* **52** 211
[4] Luo H, Greene R G and Ruoff A L 1994 *Phys. Rev.* B **49** 15341
[5] Jain C, Willis J R and Bullogh R 1990 *Adv. Phys.* **39** 127
[6] Syassen K, Christensen N E, Winzen H, Fischer K and Evers J 1987 *Phys. Rev.* B **35** 4052
[7] Khenata R, Baltache H, Rerat M, Driz M, Sahnoun M, Bouhafs B and Abbar B 2003 *Physica* B **339** 208
[8] Marinelli F, Dupin H and Lichanot A 2000 *J. Phys. Chem. Solids* **61** 1707
[9] Jha P K, Sakalle U K and Sanyal S P 1998 *J. Phys. Chem. Solids* **59** 1633
[10] Pandey R, Lepak P and Jaffe J E 1992 *Phys. Rev.* B **46** 4976
[11] Pandey R, Jaffe J E and Kunz A B 1991 *Phys. Rev.* B **43** 9228
[12] Syassen K 1986 *Physica* B + C **139** 277
[13] Zimmer H G, Winzen H and Syassen K 1985 *Phys. Rev.* B **32** 4066
[14] Hasegawa A and Yanase A 1980 *J. Phys. C: Solid State Phys.* **13** 1995
[15] Dadstani M and Pourghazi A 2006 *Phys. Rev.* B **73** 195102
[16] Zunger A, Wei S-H, Ferreira L G and Bernard J E 1990 *Phys. Rev. Lett.* **65** 353
[17] Hohenberg P and Kohn W 1964 *Phys. Rev.* B **136** 864
[18] Kohn W and Sham L J 1965 *Phys. Rev.* **140** A1133
[19] Blaha P, Schwarz K, Madsen G K H, Kvasnicka D and Luitz J 2001 *WIEN2k, An Augmented Plane Wave Plus Local Orbitals Program for Calculating Crystal Properties* Vienna University of Technology, Vienna, Austria
[20] Perdew J P, Burke S and Ernzerhof M 1996 *Phys. Rev. Lett.* **77** 3865
[21] Engel E and Vosko S H 1993 *Phys. Rev.* B **47** 13164
[22] Murnaghan F D 1944 *Proc. Natl Acad. Sci. USA* **30** 5390
[23] Zaoui A and El Haj Hassan F 2001 *J. Phys.: Condens. Matter* **13** 253
[24] Vegard L 1921 *Z. Phys.* **5** 17
[25] Jobst J, Hommel D, Lunz U, Gerhard T and Landwehr G 1996 *Appl. Phys. Lett.* **69** 97
[26] El Haj Hassan F 2005 *Phys. Status Solidi* b **242** 909
[27] Syassen K 1985 *Phys. Status Solidi* a **91** 11
[28] Dufek P, Blaha P and Schwarz K 1994 *Phys. Rev.* B **50** 7279
[29] Bachelet G B and Christensen N E 1995 *Phys. Rev.* B **31** 879
[30] El Haj Hassan F and Akdarzadeh H 2005 *Mater. Sci. Eng.* B **121** 170

[31] Charifi Z, Baaziz H and Bouarissa N 2004 *Int. J. Mod. Phys.* B **18** 137
[32] Van Vechten J and Bergstresser T K 1970 *Phys. Rev. Lett.* **31** 3351
[33] Bernard J E and Zunger A 1986 *Phys. Rev. Lett.* **34** 5992
[34] Kaneko Y and Koda T 1988 *J. Cryst. Growth* **86** 72
[35] Heyd J, Peralta J E, Scuseria G E and Martin R L 2005 *J. Chem. Phys.* **123** 1
[36] Gupta V P and Ravindra N M 1980 *Phys. Status Solidi* b **10** 715
[37] Ravindra N M, Auluck S and Srivastava V K 1979 *Phys. Status Solidi* b **93** 155
[38] Herve J P L and Vandamme L K J 1994 *Infrared Phys. Technol.* **35** 609
[39] Salem M A 2002 *Chin. J. Phys.* **41** 3
[40] Reddy R R, Kumar M R and Rao T V R 1993 *Infrared Phys.* **34** 103
[41] Moss T S, Burrel G J and Ellis B 1973 *Semiconductor Opto-Electronics* (London: Butterworths)
[42] Adachi S 1987 *J. Appl. Phys.* **61** 4869
[43] Lines M E 1990 *Phys. Rev.* B **41** 3372
[44] Swalin R A 1961 *Thermodynamics of Solids* (New York: Wiley)
[45] Ferreira L G, Wei S H, Bernard J E and Zunger A 1999 *Phys. Rev.* B **40** 3197
[46] Teles L K, Furthmuller J, Scolfaro L M R, Leite J R and Bechstedt F 2000 *Phys. Rev.* B **62** 2475
[47] Stringfellow G B 1974 *J. Cryst. Growth* **27** 21
[48] Ferhat M and Bechstedt F 2002 *Phys. Rev.* B **65** 75213
[49] Ho I-H and Stringfellow G B 1996 *Appl. Phys. Lett.* **69** 2701